PHYSICAL REVIEW A VOLUME 23, NUMBER 1 JANUARY 1981

Two-electron rearrangement K x-ray transitions in Na, Mg, and Al metals

T. Åberg, K. Reinikainen, and O. Keski-Rahkonen
Laboratory of Physics, Helsinki University of Technology, 02150 Espoo 15, Finland
(Received 28 July 1980)

One-photon $KL^n_{2,3}$ ($n = 1,2$) radiative electron rearrangement (KL^n RER) x-ray transitions have been observed in sodium, magnesium, and aluminum metals following electron-impact excitation. The structure of the KL^n RER transitions has been separated from the KLL and KL_1V radiative Auger (RA) structure and their intensity relative to the $KL^n_{2,3}$-$L^{n+1}_{2,3}$ transitions has been determined. No significant discrepancy between the experimental and calulated KL^1 RER branching ratios has been found in contrast to recent ion-impact results of Jamison *et al.* for aluminum and silicon. Our KL^2 RER results also agree with theoretical predictions.

I. INTRODUCTION

In a recent letter[1] Jamison *et al.* reported strong polarization of the KL^1 RER (radiative electron rearrangement) x-ray satellite in thick Al and Si targets which were bombarded with 2-MeV He^+ ions. This result is in accordance with the previously observed polarization of the Al $K\alpha'$ satellite following bombardment by H^+, He^+, and Li^+ ions.[2,3] The polarization of both KL^1 RER and $K\alpha'$ has been attributed to the alignment of the initial $1s^{-1}2p^{-1}\,{}^1P$ magnetic substates with respect to the beam axis.[1-5] Since KL^1 RER and $K\alpha'$ have common initial states their intensity ratio should be independent of the polarization and the angle of observation. Using this property Jamison *et al.*[1] also measured the KL^1 RER to $K\alpha'$ intensity ratio for 2-MeV He^+ impact. Their results, 0.014 ± 0.003 (Al) and 0.013 ± 0.003 (Si), do not accord with previous ion-impact measurements[6] and with the theory[7] of KL^n RER transitions which predicts branching ratios twice as large.

The extraction of the KL^n RER intensity distributions from the background is a very complex problem. Hence we have used a semiempirical separation procedure which is based on justified assumptions regarding the position and shape of the KL^n RER multiplets. As a result, not only the relative KL^n RER energies and intensities are obtained but the KL_1V RA structures are identified as well. In Na there are no previous observations of the KL^n RER transitions and in Mg the KL^1 RER line is identified correctly for the first time. We regard our Na KL^1 RER result as the most reliable of the three metals since the background consists of the slowly varying slope of the KLL RA (radiative Auger) continuum.

We have used electron excitation of thick targets. Thus the resulting alignment of the initial KL^n states is very small, as will be shown in detail for the $1s^{-1}2p^{-1}\,{}^1P$ states. The contribution of the $1s^{-1}2s^{-1}$ states to the KL^n-L^{n+1} transitions is also shown to be small in comparison with the $1s^{-1}2p^{-1}$ contribution. Hence our results are comparable to the calculated KL^n RER intensities which are given with respect to the intensity of $KL^n_{2,3}$-$L^{n+1}_{2,3}$ transitions.[7]

II. EXPERIMENTAL RESULTS

K x-ray spectra were recorded with a Bragg plane-crystal spectrometer equipped with two Soller collimators (0.075° and 0.15°). A gypsum analyzing crystal ($2d = 1.5217$ nm) was used for Na and an ADP (ammonium dihydrogen phosphate) crystal ($2d = 1.0634$ nm) for Mg and Al. The detector and recording system were as earlier.[8]

For the electron-impact measurements two separate x-ray tubes built in our laboratory were used. The first version could be pumped with an ion pump down to about 1 μ Pa. It was operated at 6 kV $\times$10 mA and had a resistance-heated crucible which was loaded with metallic 99.9% pure Na for evaporation of a Na film *in situ* on an Al anode substrate. The oxidation of the Na sample was monitored by measurements of the $K\beta$ valence-band region in which separate peaks are observed for metal and oxide. A fresh deposited layer contained 10% to 15% Na_2O. A 20% limit was exceeded typically within two days after which a new evaporation was carried out.

The second x-ray tube which was used for the Mg and Al measurements was operated at 12 kV $\times$ 10 mA. It was equipped with a liquid-nitrogen cold trap and a diffusion pump charged with a diphenyl ether fluid. Pressures below 0.1 μPa could be obtained. Anodes were machined from pure (Mg: 99.8%; Al: 99.999%) metal rods and cleaned mechanically immediately before inserting into the vacuum. From inspection of the $K\beta$ structures no traceable oxidation was observed within one week.

Measured spectra are shown in Fig. 1. They are corrected for counter dead time, crystal dis-

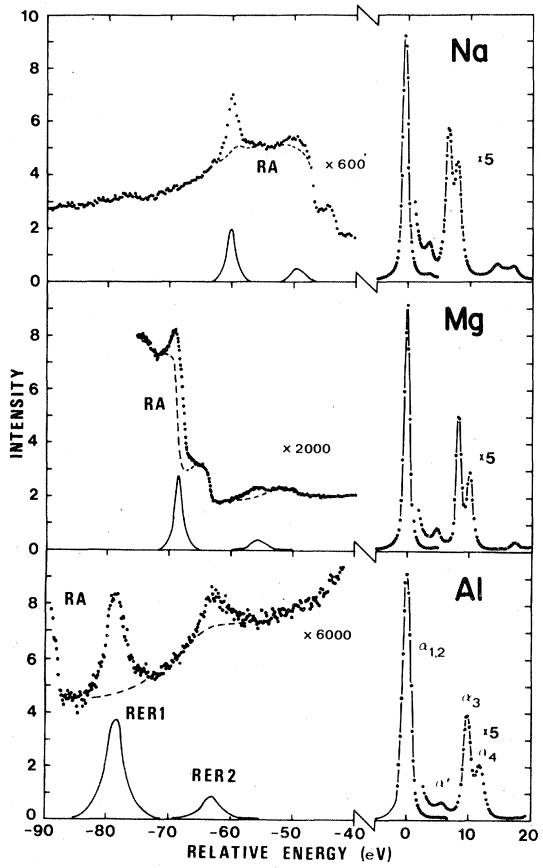

FIG. 1. Corrected spectra in the KL^n RER ($n=1,2$) region together with the $K\alpha_{1,2}$ line and the $KL^1(\alpha', \alpha_3, \alpha_4)$ high-energy satellites are shown by points. The positions and relative intensities of the KL^n RER lines (RER 1 and 2), drawn separately in full line, have been obtained as explained in Sec. II. The residual spectra indicated by the dashed line are mostly due to the KLL and KL_1V radiative Auger (RA) structures. In Mg and Al the KL^2 RER lines are situated on the slopes of the KL_1V RA structures with onsets at approximately −48 and −55 eV, respectively.

persion and reflecting power, as well as for the transmission of the x-ray tube and detector windows. A careful fluorescence analysis of the samples did not reveal any impurity lines interfering with the observed structures.

Since the spectral distribution is complex in the region of the KL^n RER transitions, they were separated from the other features using an interactive computer code together with a graphic display. The heights and positions of the lines to be fitted were varied until the adjustment became satisfactory on the display. This procedure is naturally not unique but it leads to plausible results for the relative integrated intensities and for the positions of lines with separable maxima.

The relative positions of the KL^1 RER and KL^2 RER satellites are given in Table I and the relative intensities in Tables II and III. The theoretical energies were calculated for Ne-like ions using a multiconfigurational Hartree-Fock (MCHF) code by Froese Fischer.[9] In addition, indirect experimental energies were obtained from known x-ray and Auger[10,11] energies using the formula

$$\Delta E(KL^1\ \mathrm{RER}) = E(K\alpha_4) - E(K\alpha_{1,2}) + E(KL_1L_1, {}^1S) - E(KL_2L_3, {}^1D)\,. \quad (1)$$

They provide initial estimates of the positions. Using the fitting procedure the KL^1 RER energies and intensities were obtained first. The initial profile of KL^1 RER in Mg was obtained by scaling from the Al KL^1 RER line since in Mg the KL^1 RER is situated on the steep slope of the KL_2L_3 ^1D RA threshold. This may be the reason why Jamison *et al.*[6] erroneously identified the KL_2L_2 ^1S RA threshold at −74 eV as the KL^1 RER line.

A synthetic KL^2 RER profile was formed by adding two experimental KL^1 RER profiles at calculated positions with the statistical weights $^2P:{}^2D = 9:5$.[7] The ^2S component was ignored due to its small statistical weight. The initial estimates of the positions were obtained by adding the

TABLE I. KL^n RER x-ray transition energies relative to the $K\alpha_{1,2}$ line (in eV).

	KL^1 RER			KL^2 RER		
		Experiment		Theory[b]		
Target	Theory[a]	This work	Eq. (1)	^2P	^2D	^2S
Na	−62.4	−59.4(2)	−59.6(4)	−47.9	−49.0	−45.0
Mg	−70.7	−68.3(4)	−69.2(3)	− 3.6	−54.4	−49.8
Al	−79.1	−78.9(2)	−79.5(3)	−58.1	−59.9	−54.6

[a]Hartree-Fock calculations using a program of Froese Fischer (Ref. 9). In the final state the $2s^{-2}$ and $2p^{-2}$ configurations were mixed.

[b]The ^2S energies were from multiconfiguration Hartree-Fock calculations with the $1s^{-1}\,2p^{-2} - 1s^{-1}\,2s^{-2}$ mixing included. In the final state the $2s^{-2}\,2p^{-1}$, and $2p^{-3}$ configurations were mixed.

TABLE II. Relative intensities of KL^1 RER x-ray transitions (in %).

	$I(KL^1$ RER$)/I(KL^1)$				
		Experiment		Theory	
Target	This work	Reference 1 [a]	Reference 6 [b]	Reference 7	This work [c]
Na	0.20(3)			0.18	0.21
Mg	0.13(4)			0.18	0.18
Al	0.13(3)	0.09(2)		0.17	0.15
Si		0.09(2)	0.20(4)	0.17	

[a] The experimental $I(KL^1$ RER$)/I(K\alpha')$ ratios have been multiplied by the statistical factor $\frac{1}{15}$.
[b] Excluding excitations with ions having $Z \leq 6$ in accordance with Ref. 3.
[c] The theoretical values of Ref. 7 have been corrected for measured nonstatistical $N(^3P)/N(^1P)$ electron-impact ratios as explained in Sec. III A.

theoretical KL^2-KL^1 RER energy differences to the experimental positions of the KL^1 RER lines. In the fitting procedure the KL^2 RER shapes were kept frozen and only the height and the position of the whole profiles were varied until consistency was achieved. In Na the KL^2 RER sits on the $KL_2L_{2,3}$ ^1S and ^1D thresholds. In Mg and Al the KL^2 RER multiplets interfere with the KL_1V RA structure, the position of which can be estimated from corresponding Auger electron energies.[10,11] For the fitting purposes the shape of the KL_1V slope was assumed smooth, similar to the KLL RA structures. As shown by Table III the error limits of the KL^2 RER intensities are quite large due to the extraction difficulties. The KL_1V RA intensity is approximately 1% relative to the KL^2-L^3 transitions in Mg and Al.

III. COMPARISON WITH ION-ATOM COLLISION EXPERIMENTS AND WITH THEORY

A. Dependence of relative intensity on the excitation mode

When randomly oriented target atoms are excited by a collimated beam of particles, the excited atoms usually align themselves with respect to the beam axis. As a consequence, the resulting radiation is anisotropic. In the dipole approximation the intensity pattern of a multiplet of an N_e-electron system is given by

$$I(\Theta, \Psi, \beta) = I_0[1 + kf(\Theta, \Psi, \beta)], \tag{2}$$

TABLE III. Relative intensities of KL^2 RER x-ray transitions (in %).

	$I(KL^2$ RER$)/I(KL^2)$		
	Experiment		Theory
Target	This work	Reference 6	Reference 7
Na	0.57(17)		0.54
Mg	0.34(10)	0.35(8)	0.53
Al	0.40(15)	0.41(10)	0.51
Si		0.50(6)	0.50

where

$$I_0 = (2S+1) \sum_{M_L' M_L} N(M_L) \left| \left\langle M_L' \left| \sum_{\nu=1}^{N_e} r_\nu \right| M_L \right\rangle \right|^2 \tag{3}$$

accounts for the populations $N(M_L)$ of the initial magnetic substates in an average fashion. The function $f(\Theta, \Psi, \beta)$ is given by

$$f(\Theta, \Psi, \beta) = P_2(\cos\Theta) - \tfrac{3}{2}\sin^2\Theta \cos 2\Psi \cos 2\beta, \tag{4}$$

where Θ is the angle between the direction of observation and the beam axis.[12] As described in detail in Ref. 12 the angles Ψ and β account for the polarization selected by the detector. The parameter k includes the influence of the initial populations and fine structure on the radiation pattern.

In their works Jamison *et al.*[1-3] considered two intensities, $I_\parallel$ and $I_\perp$, which correspond to, respectively, $\Theta = 90°$, $\Psi = 0°$, and $\Theta = \Psi = 90°$ in Eq. (4). The use of a crystal spectrometer as a polarimeter introduced the factor $\tan\beta = \cos 2\Theta_B$, where Θ_B is the Bragg angle of the appropriate reflection from the analyzing crystal.

Ideally we measure $I_\parallel$ in our experiments, but since we excite thick targets with electrons instead of ions, Θ and Ψ are not well-defined angles. Consequently, we observe a weighted average of $I(\Theta, \Psi, \beta)$ in which the weight is a complicated function of the penetration depth but may roughly be approximated by a $\cos^2\Theta$ distribution.[13] Hence our results are closer to I_0 than Eq. (2) anticipates.

Both KL^1 RER and $K\alpha'$ are $^1P_1$ to $^1S_0$ transitions for which k in Eq. (2) is given by

$$k = \frac{Q_1 - Q_0}{2Q_1 + Q_0}, \tag{5}$$

where the initial populations $N(|1|)$ and $N(0)$ have been replaced by the corresponding excitation probabilities Q_1 and Q_0, respectively. For 2-MeV He^+ impact both experiments[1-3] and calculations[4,5] indicate that $Q_0/Q_1 \simeq 3$, i.e., $k \simeq -\frac{2}{5}$ or $I_\parallel/I_\perp \simeq 3$ for $\Theta_B = 90°$. For 6 keV (Na) and 12 keV (Mg, Al)

electron impact the situation is entirely different. Since the electron energies are initially six to ten times larger than the threshold energy, the $1s^{-1}2p^{-1}$ double excitation can be described adequately by the shake concept.[14] Consequently, $Q_0 \simeq Q_1$ since the shake probability is independent of M_L and the primary $1s$ ionization is isotropic. For electron but not ion impact one may argue on semiclassical grounds that any alignment associated with the residual direct collision mechanism cannot exceed that of the $2p$ ionization which is known to be small[15] in the energy range of interest. Using data of Ref. 15 and the appropriate depolarization factor[16] for the $2p^{-1}$ states, one may conclude that if the direct collisions were solely responsible for the $1s^{-1}2p^{-1}$ excitation, then $k \lesssim 0.02$. Hence it is clear from Eqs. (2) and (3) that our electron impact data correspond to I_0 in which $N(0) = N(|1|)$.[17]

Our conclusions with regard to the isotropy of KL^1 RER and $K\alpha'$ apply also to the ^3P-$^3PK\alpha_3$ multiplet for which $k = -\frac{1}{2}D\,k(\alpha')$, where D is the appropriate depolarization factor[16] and to the ^1P-$^1D\,K\alpha_4$ multiplet for which $k = \frac{1}{10}k(\alpha')$. However, although $N(0) = N(|1|)$ for both ^1P and ^3P $1s^{-1}2p^{-1}$ states $N(^1P)$ may not necessarily be equal to $N(^3P)$ for a given M_L.[7] As a measure of the $N(^3P)/N(^1P)$ ratio we may take the ratio of $K\alpha_3$ and $K\alpha_4$ which is given by

$$\frac{I(K\alpha_3)}{I(K\alpha_4)} = \frac{9N(^3P)}{5N(^1P)} = \frac{9Q(^3P)\Gamma(^1P)}{5Q(^1P)\Gamma(^3P)} \tag{5}$$

in the frozen-core approximation. Since the decay probabilities $\Gamma(^3P)$ and $\Gamma(^1P)$ are approximately equal,[7] any significant deviation from the statistical ratio 9 : 5 would indicate a nonstatistical excitation. From our Na measurements and the Mg and Al measurements of Krause and Ferreira[18] at 6 to 12 keV we obtain the following $N(^3P)/N(^1P)$ ratios: 0.76 ± 0.02 (Na), 0.99 ± 0.04 (Mg), and 1.29 ± 0.04 (Al). Hence the calculated $I_0(KL^1\ \text{RER})/I_0(KL_{2,3}\text{-}L^2_{2,3})$ ratios which are given in Table II, based on the assumption of statistical initial state populations,[7] i.e., $N(^3P)/N(^1P) = 1$, should be corrected in the case of Na and Al. The corrected nonstatistical branching ratios of Na and Al are 0.21 and 0.15, respectively. Unfortunately, a similar analysis is not possible for KL^2 RER transitions. However, the KL^2 RER branching ratio would not be very sensitive to any deviations from the term independence.[7]

In the He^+-impact case it is more appropriate to consider $I(KL^1\ \text{RER})/I(K\alpha')$ (Ref. 1) in accordance with Eq. (2) and the arguments given above. For projectiles heavier than oxygen, the anisotropy of KL^1 RER and $K\alpha'$ is probably smaller than that for He^+, and for KL^2 RER it is negligible in general.[1,3] Hence we have included the corresponding data from Ref. 6 in Tables II and III for comparison with the theory.

There is another source of uncertainty influencing the comparison between theory and experiment, namely the overlap between KL_1-$L_1L_{2,3}$ and $KL_{2,3}$-$L^2_{2,3}$ transitions. According to transition operator calculations[19] the $1s^{-1}2s^{-1}\,^1S$-$2s^{-1}2p^{-1}\,^1P$ $K\alpha''$ transition overlaps $K\alpha'$ and the $1s^{-1}2s^{-1}\,^3S$-$2s^{-1}2p^{-1}\,^3P$ $K\alpha_3'$ transition $K\alpha_3$ and $K\alpha_4$ in Ne and Si. In particular, $\Delta E(K\alpha' - K\alpha'') = -0.3$ eV for Ne and +0.2 eV for Si. Hence a complete separation of these two groups is experimentally impossible. On the other hand, an appreciable fraction of the KL_1 states decay into $KL_{2,3}V$ states by $L_1L_{2,3}V$ Coster-Kronig transitions.[7] Nevertheless, as shown below especially the weak $K\alpha'$ line may interfere seriously with the rather broad $K\alpha''$ line.

For ion impact the ratio of $1s^{-1}2s^{-1}$ to $1s^{-1}2p^{-1}$ excitations can be estimated from semiclassical calculations of atomic Coulomb excitation.[20] According to Hansteen and Mosebekk[21]

$$Q(KL_1)/Q(KL_{2,3}) \cong 3 \lim_{b \to 0} [I_b(2s)/I_b(2p)],$$

where $I_b(nl)$ is the Coulomb ionization probability of any of the nl electrons at the impact parameter value b. For 2-MeV He^+ (0.5-MeV H^+) on Al this ratio is 1.17 according to calculations with screened hydrogenic wave functions.[20] Consequently,

$$\frac{I_0(K\alpha'')}{I_0(K\alpha')} = \frac{3Q(KL_1)\Gamma(KL_{2,3})}{2Q(KL_{2,3})\Gamma(KL_1)}\left(1 + \frac{\Gamma(L_1)Q(KL_1)}{3\Gamma(KL_1)Q(KL_{2,3})}\right)^{-1} \tag{6}$$

is about 0.46 if we assume that $\Gamma(L_1) \cong 2\Gamma(K)$.[22] In Eq. (6), which is independent of the $N(0)/N(|1|)$ ratio, the factor $\frac{3}{2}$ accounts for the ratio of the multiplet strengths and the half-width Γ for the lifetimes of the initial vacancies. The decay of $1s^{-1}2s^{-1}$ states into $1s^{-1}2p^{-1}$ states by $L_1L_{2,3}V$ Coster-Kronig transitions has also been taken into account.

According to our estimates given above, a complete overlap between $K\alpha''$ and $K\alpha'$ would yield an experimental $r_\perp = I_\perp(KL^1\ \text{RER})/I_\perp(K\alpha')$ ratio which is too small by 43% for $Q_0/Q_1 = 3$. The corresponding value for $r_\parallel$ is 22% which is less than that of $r_\perp$ since $K\alpha''$ is isotropic. Although this may be one of the reasons why the measured $r_\perp$ and $r_\parallel$ values of Ref. 1 are significantly smaller than the calculated value,[7] one should note that according to the experiments[1] $r_\perp$ and $r_\parallel$ agree within ±15% for both Al and Si.

For electron impact we may obtain a similar estimate of $I_0(KL_1)/I_0(KL_{2,3})$ from

$$\frac{I_0(KL_1)}{I_0(KL_{2,3})}=\frac{6W(2s)\Gamma(KL_{2,3})}{5W(2p)\Gamma(KL_1)}\left(1+\frac{\Gamma(L_1)W(2s)}{\Gamma(KL_1)W(2p)}\right)^{-1}, \tag{7}$$

where $W(nl)$ is the probability[23] that any of the nl electrons is shaken from its orbit in the $1s$ ionization process. The ratio (7) is about 5% according to Hartree-Fock calculations of $W(nl)$.[23] Hence we may neglect the KL_1 states in our analysis of the electron-impact measurements of KL^1 RER and also KL^2 RER.

B. Remarks on theory

The theoretical intensity values listed in Tables II and III are obtained from Ref. 7. They are based on a two-configuration interaction model which attributes the KL^n RER satellites to the mixing between the quasidegenerate $2p^{-m}$ and $2s^{-2}2p^{-m+2}$ L-shell configurations in the initial $(m=n)$ and final $(m=n+1)$ states. The adequacy of this model was tested by considering the stability of the $2s$-$2p$ mixing against the influence of the L-shell correlation.[7] The contribution from the relaxation during x-ray emission was also found to be small. In the following we consider only the KL^1 RER satellite and examine whether the branching ratio could be affected significantly by any additional configuration-mixing effects in the initial and final states. Reasonable criteria for the choice of the configurations are the following: (i) They should differ from the principal Hartree-Fock configurations, $1s2s^22p^5(^1P)$ and $1s^22s^02p^6(^1S)$, by two-electron excitations in both states in accordance with Brillouin's theorem for single determinants.[24] (ii) Each additional initial-state configuration should be connected to the final-state principal configuration by a one-electron dipole transition matrix element and vice versa. The requirements (i) and (ii) determine uniquely the wave functions which are

$$\begin{aligned}\Psi_i&=a_0\phi(1s2s^22p^5,{}^1P)+\sum_{\mu=1}^{\infty}\sum_{l=0,2}a_\mu(l)\phi(1s^22s^02p^5\mu l,{}^1P),\\ \Psi_f&=b_0\phi(1s^22s^02p^6,{}^1S)+b_1\phi(1s^22s^22p^4,{}^1S)\\ &\quad+b_2\phi(1s^02s^22p^6,{}^1S)+\sum_{\nu=3}^{\infty}b_\nu\phi(1s2s2p^5\nu p,{}^1S).\end{aligned} \tag{8}$$

The summation over μ and ν includes the continuum. In the calculations of Ref. 7, $a_\mu=0$ $(\mu\geq 1)$ and $b_\nu=0$ $(\nu\geq 2)$.

According to Eq. (8) the additional configurations involve electron transfer to or from the K shell. Hence they are expected to be small in comparison with b_1. This can be seen explicitly from first-order perturbation theory which gives

$$\frac{b_2}{b_1}=\left(\frac{\epsilon_{2p}-\epsilon_{2s}}{\epsilon_{1s}-\epsilon_{2s}}\right)\frac{G^0(2s1s)}{G^1(2s2p)}\sqrt{3} \tag{9}$$

and omitting geometrical factors and the exchange part

$$\frac{b_\nu}{b_1}\simeq\left(\frac{\epsilon_{2p}-\epsilon_{2s}}{\epsilon_{1s}-\epsilon_{\nu p}}\right)\frac{R^0(2s\,\nu p\,1s\,2p)}{G^1(2s2p)}. \tag{10}$$

Using known values of orbital energies ϵ and Slater integrals G^k (Ref. 25), as well as relationships between G^k and R^k integrals, one may estimate that $|b_\nu/b_1|<|b_2/b_1|\simeq 10^{-2}$ in Al. The coefficients

$$a_\mu(l)\simeq\frac{R^0(2s\,2s\,1s\,\epsilon l)}{2\epsilon_{2s}-\epsilon_{1s}-\epsilon_{\mu l}}\,\delta_{l,0} \tag{11}$$

are smaller than b_2 for low μ but become singular at $\epsilon_{\mu l}=\epsilon_{KL_1L_1}$. The singularity is a manifestation of real and virtual processes in which the initial $1s^{-1}2p^{-1}\,{}^1P$ states decay by the ejection of an electron which by recombination with the atom emits a photon.[26] The probability amplitudes of such processes are generally expected to be very small but exceptions exist among x-ray transitions.[27] If we assume that the interaction matrix elements are nearly constant in the vicinity of $\epsilon=\epsilon_{KL_1L_1}$, then only the imaginary part related to the real process enters. In this case the magnitude of

$$z=\frac{6\pi D_1(2p\epsilon s)R^0(2s\,2s\,1s\,\epsilon s)(\epsilon_{2p}-\epsilon_{2s})}{\sqrt{2}\,G^1(2s2p)D_1(1s2p)} \tag{12}$$

in comparison to unity gives an estimate of the importance of the initial-state mixing.[27] From known values of dipole matrix elements D_1 and the Slater integrals G^1 and R^0 we obtain $z\lesssim 3\times 10^{-3}$ in Al. Hence among all configurations which are connected to the principal configurations by first-order dipole interactions, only the final-state $1s^22s^22p^4$ configuration seems to contribute significantly to the KL^1 RER probability amplitude.

IV. CONCLUSION

Our analysis of electron-impact measurements of the KL^n RER $(n=1,2)$ satellites in Na, Mg, and Al leads to a consistent picture with regard to the origin of these transitions. The measured intensities agree well with the theory, especially when a semiempirical correction for nonstatistical populations of the initial terms is introduced. It is found that our electron-impact data of the $I(KL^1\text{ RER})/I(KL^1)$ ratio are neither affected by anisotropy corrections nor by overlap between KL_1-$L_1L_{2,3}$ and $KL_{2,3}$-$L^2_{2,3}$ transitions in contrast to recent light-ion impact results.

ACKNOWLEDGMENTS

We would like to thank Professor Patrick Richard for helpful comments and Esko Mikkola for his assistance. This work was supported by the Finnish Academy of Sciences.

[1]K. A. Jamison, J. Newcomb, J. M. Hall, C. Schmiedekamp, and P. Richard, Phys. Rev. Lett. 41, 1112 (1978).
[2]K. A. Jamison and P. Richard, Phys. Rev. Lett. 38, 484 (1977).
[3]K. A. Jamison, P. Richard, F. Hopkins, and D. L. Matthews, Phys. Rev. A 17, 1642 (1978).
[4]L. Kocbach and K. Taulbjerg, in *Abstracts of Papers of the Tenth International Conference on the Physics of Electronic and Atomic Collisions, Paris, 1977* (Commisariat à l 'Energie Atomique, Paris, 1977), p. 44.
[5]E. Merzbacher and J. Wu, in Ref. 4, p. 46.
[6]K. A. Jamison, J. M. Hall, I. Oltjen, C. W. Woods, R. L. Kauffman, T. J. Gray, and P. Richard, Phys. Rev. A 14, 937 (1976).
[7]T. Åberg, K. A. Jamison, and P. Richard, Phys. Rev. A 15, 172 (1977).
[8]E. Mikkola, O. Keski-Rahkonen, and R. Kuoppala, Phys. Scr. 19, 29 (1979).
[9]C. Froese Fischer, Comput. Phys. Comm. 14, 145 (1978).
[10]P. M. Th. M. van Attekum and J. M. Trooster, J. Phys. F 8, L169 (1978).
[11]A. Barrie and F. J. Street, J. Electron Spectrosc. Relat. Phenom. 8, 23 (1976).
[12]U. Fano and J. H. Macek, Rev. Mod. Phys. 45, 553 (1973).
[13]V. Lantto, J. Phys. D 7, 703 (1974).
[14]T. Åberg, in *Proceedings of the International Conference on Inner Shell Ionization Phenomena and Future Applications, Atlanta, 1972*, edited by R. W. Fink, S. T. Manson, J. M. Palms, and P. V. Rao (U.S. GPO, Washington, D.C., 1973), p. 1509.
[15]M. Rødbro, R. DuBois, and V. Schmidt, J. Phys. B 11, L551 (1978).
[16]W. Mehlhorn and K. Taulbjerg, J. Phys. B 13, 445 (1980).
[17]In a measurement the variation of the Al $K\alpha'$ intensity as a function of θ was found to be within ±10% for an electron-impact energy of 12 keV (E. Mikkola, unpublished results).
[18]M. O. Krause and J. G. Ferreira, J. Phys. B 8, 2007 (1975).
[19]G. Howat, O. Goscinski, and T. Åberg, Physica Fenn. Suppl. S1, 9, 241 (1974) and unpublished results.
[20]J. M. Hansteen, O. M. Johnsen, and L. Kocbach, At. Nucl. Data Tables 15, 305 (1975).
[21]J. M. Hansteen and O. P. Mosebekk, Phys. Rev. Lett. 29, 1361 (1972).
[22]M. O. Krause and J. Oliver, J. Phys. Chem. Ref. Data 8, 329 (1979) report the following widths: 0.42 eV (K) and 0.73 eV (L_1); H. Neddermeyer, Phys. Rev. B 13, 2411 (1976) measured 0.47 eV for K linewidth; and P. H. Citrin, G. K. Wertheim, and Y. Baer, *ibid.* 16, 4256 (1977) obtained 0.78 eV for L_1 linewidth.
[23]T. Åberg, Ann. Acad. Sci. Fen. Ser. A VI, 308, 1 (1969).
[24]C. Froese Fischer, *The Hartree-Fock Method for Atoms* (Wiley, New York, 1977), Sec. 2.5.
[25]J. B. Mann, Los Alamos Scientific Report No. LA-3690 (unpublished).
[26]T. Åberg, Phys. Scr. 21, 495 (1980).
[27]H. P. Kelly, Phys. Rev. Lett. 37, 386 (1976); M. Ya. Amusia, I. S. Lee, and A. N. Zinoviev, Phys. Lett. 60A, 300 (1977).